Quantitative Evaluation of Brain Magnetic Resonance Images Using Voxel-based Morphometry and Bayesian Theorem for Patients with Bipolar Disorder

Yong-Sheng Chen[1] Li-Fen Chen[2,3,*] Ya-Ting Chang[1] Yung-Tien Huang[1]

Tong-Ping Su[4,5] Jen-Chuen Hsieh[2,3]

[1]*Institute of Computer Science, National Chiao Tung University, Hsinchu 300, Taiwan, ROC*
[2]*Institute of Brain Science, National Yang-Ming University, Taipei112, Taiwan, ROC*
[3]*Department of Medical Research and Education, Taipei Veterans General Hospital, Taipei 112, Taiwan, ROC*
[4]*Division of Psychiatry, School of Medicine, National Yang-Ming University, Taipei 112, Taiwan, ROC*
[5]*Psychiatry Department, Taipei Veterans General Hospital, Taipei 112, Taiwan, ROC*

Received 22 Jul 2008; Accepted 14 Aug 2008

Abstract

The present diagnosis of bipolar disorder (BD), which mainly depends on patients' symptoms and self reports of past history and mood status, may encounter difficulty of distinguishing from unipolar disorder when patients behave depressively in clinic. This work proposes a novel computer-aided evaluation system for bipolar disorder using anatomic magnetic resonance images (MRI) to provide a second opinion for clinician's diagnosis. First we adopt the voxel-based morphometry method to identify brain regions with significant difference between patient and normal control groups as regions of interest (ROIs). Then the MRI data within these ROIs are processed with principal component analysis (PCA) in order to reduce feature dimensionality. Finally, a classification model based on Bayesian theorem together with Parzen-window density estimation in PCA space is constructed to provide the possibility of an individual belonging to the BD patient group. The proposed system reaches 86.8% accuracy in classification. In our experiment, the misdetection rate was zero, and the false alarm was 15.8%. Through appropriate feature analysis and selection method, this computer-aided system can detect the disease of BD and obtain high classification accuracy.

Keywords: Bipolar disorder, Magnetic resonance images (MRI), Principle component analysis, Voxel-based morphometry, Classification, Bayesian model

1. Introduction

Currently, diagnoses of psychiatric diseases are determined mainly according to patients' symptoms and self-report of past history and mood status. Clinician assessments including structured clinical interview are further needed for concordance with self-report. The guidebook, Diagnostic and Statistical Manual (DSM) of Mental Disorders-IV, is the most popular handbook for psychiatrists' reference. Whereas it would be problematic employing a symptom-based rather than an etiologically based approach [1], the research agenda for DSM-V (a release of the final, approved DSM-V is expected in May, 2012.) emphasizes the need of a new classification system for psychiatric disorders from translated basic and clinical neuroscience research findings. Phillips and Frank suggested that sophisticated neuroimaging and genetic research has deepened the understanding of the neurobiology of bipolar disorder [1].

Among multiple neuroimaging modalities, magnetic resonance images (MRI) have been widely used for classifying anatomical abnormality in human brains non-invasively [2-6]. For example, Pardo *et al.* adopted linear discriminant analysis to classify the difference between adolescent schizophrenia and bipolar disorders using both MRI and neuropsychological tests of subjects [2]. In [4], Fan *et al.* combined structural and functional information extracted from MRI data to establish a computer-aided evaluation system which, providing objective quantitative indices based on those modalities, may be helpful for diagnosis. Kawasaki *et al.* presented another classification approach for schizophrenia based on multivariate linear model which was built from gray matter concentration [5]. Similarly, Yoon *et al.* proposed a pattern classification method based on principal components of cortical thickness from MR images

* Corresponding author: Li-Fen Chen
Tel: +886-2-28267384; Fax: +886-2-28273123
E-mail: lfchen@ym.edu.tw

between schizophrenic patients and healthy controls [6].

In the computational neuroanatomy field, voxel-based morphometry (VBM) is an emerging method which compares brain volume difference between two groups in a voxel-by-voxel manner [7-8]. It provides thorough and neuroanatomical information to distinguish healthy from diseased brains. In the literature, several kinds of neuropsychiatric diseases have been studied using the VBM technique, e.g. attention-deficit hyperactivity disorder, obsessive-compulsive disorder, schizophrenia, and bipolar disorder [5,9-12]. Among these diseases, bipolar disorder (BD) is a kind of mood disorder with unusual shifts in a person's mood, energy, and ability to function cognitively. Such periodical mood swings between depressive episodes and manic episodes cause functional and structural impairments of diseased brains [13-15]. The present diagnosis, which mainly depends on patients' symptoms and self report of past history and mood status, may encounter difficulty of distinguishing from unipolar disorder when patients behave depressively in clinic.

This work proposes a novel computer-aided evaluation system using anatomic MR images to estimate probability of diseased individual brain to provide a second opinion for clinical diagnosis. Since numerous studies have shown abnormality of brain regions between healthy and BD patients [16-22], in the first step, we adopted the VBM method to identify brain regions with significant difference between two groups as regions of interest (ROIs). Then the MRI data within these ROIs were concatenated and processed with principal component analysis (PCA) in order to reduce feature dimensionality. Finally, the classification model based on Bayesian theorem together with Parzen-window density estimation in PCA space was constructed and used to provide the possibility of an individual being a BD patient.

2. Materials and methods

2.1 Subjects

Fifteen BD patients during euthymic phase (five males, mean age=37.2 ± 12.1 y/o) were selected from the outpatients of the psychiatry department of Taipei Veterans General Hospital. The clinical diagnosis had been made by two independent psychiatrists using DSM-IV-TR. The mean illness duration was 8.4±5.5 years. All patients were taking a range of medications, including antimanic (n=1), anticonvulsant (n=11), antidepressant (n=6), and antipsychotic (n =5). Seventy-six healthy subjects (34 males, mean age = 27.9 ± 11.5 y/o) were recruited through advertisement from the community. Inclusion criteria for these healthy subjects consisted of 1) absence of a history of axis I psychiatric conditions in first-degree relatives reported, 2) absence of axis I psychiatric conditions, including substance dependence, current substance abuse, or major medical conditions. All subjects provided written informed consent to participate in the study according to the guidelines approved by the Institutional Committees of Medical Ethics and Radiation Safety.

2.2 MRI acquisition

Each participant was scanned on a 1.5-T GE MRI scanner (Signa; GE Healthcare, Milwaukee, Wisconsin) by means of a standard 30-cm circularly polarized head coil. Using a three-dimensional sequence (fast spoiled gradient-echo acquisition in the steady state), 124 contiguous T1-weighted 1.5-mm axial images across the entire brain were collected (TE = 1.828 ms, TR = 8.54 ms, flip angle = 15°; FOV = 26 × 26 × 10 cm^3; matrix size = 256 × 256), yielding a voxel size of 1.02 × 1.02 × 1.50 mm^3.

2.3 System summary

Figure 1 illustrates the flowchart of the proposed MRI computer-aided evaluation system. The procedure in this work consisted of three steps: ROI determination, feature selection, and model learning. In the first step, the VBM approach was applied to differentiate structural abnormalities between BD patients and control subjects. A threshold (p<.001) was set in the VBM results to determine the ROIs in MRI volume data as classification feature. Secondly, PCA was applied to reduce the dimension of feature space obtained from the ROIs. In the last step, we adopted Parzen window technique to estimate the probability density function for each group. Bayesian theorem was then used to provide the possibility of an individual being a BD patient. The details of each step are described in the following.

2.4 ROI determination

In order to determine brain regions with significant difference between healthy subjects and BD patients, we chose part of the data (healthy n=30, BD patients n=15, gender- and age-matched) for VBM study. The VBM procedure we applied was as follows: 1) non-brain tissues in MR images were removed using the Brain Extraction Tool v2 in the FSL toolbox [23]; 2) the images without non-brain tissues were segmented by FMRIB's Automated Segmentation Tool into gray matter (GM), white matter (WM), and cerebrospinal fluid (CSF) images in native space; 3) all GM, WM, and CSF images were normalized, respectively, to the ICBM152 template by SPM2 software (Wellcome Trust Centre for Neuroimaging, London, UK), implemented in MATLAB 7.0 (Mathworks Inc., Sherborn, MA, USA), and then averaged to construct customized GM, WM, and CSF templates; 4) each GM, WM, and CSF image in native space was normalized to the corresponding GM, WM, and CSF customized templates in a stereotactic space; 5) modulation and smoothing with an 8 mm FWHM isotropic Gaussian kernel were applied to each image; and 6) finally, two-sample t-test was performed on the modulated images to produce a t-map for indicating regional discrepancy between patient and control groups. After the VBM processing, a threshold (p<.001) was set for the resulting t-map to build up three mask for GW, WM, and CSF tissues, respectively, as ROIs. All voxels within ROIs were concatenated to form a high-dimensional feature vector.

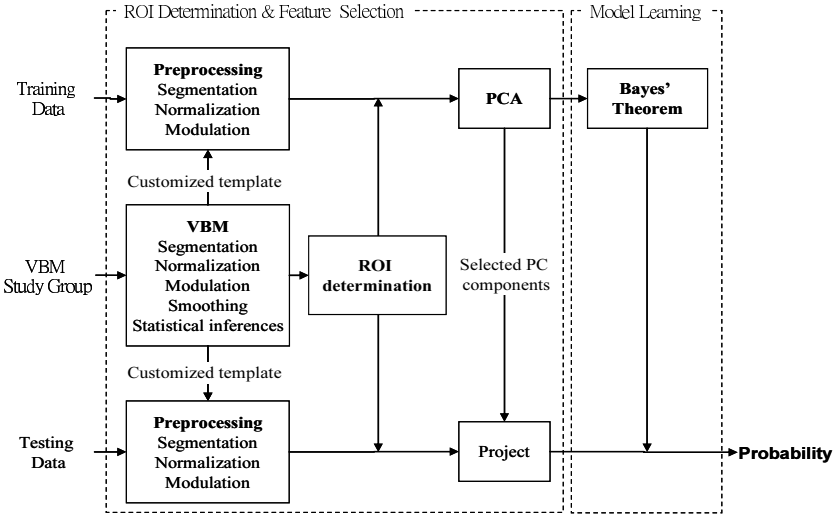

Figure 1. Flowchart of the proposed MRI-based computer-aided evaluation system.

2.5 Feature selection

Let $y=\{y_1, y_2,\ldots, y_n\}$ represent feature vectors for n subjects. The mean $\bar{y}$ and scatter matrix S can be calculated as follows:

$$\bar{y} = \frac{1}{n}\sum_{i=1}^{n} y_i \tag{1}$$

$$S = \sum_{i=1}^{n} (y_i - y)(y_i - y)^T \tag{2}$$

After PCA was applied, we get

$$SE=DE \tag{3}$$

where the diagonal matrix D holds eigenvalues of S and the column vectors of $E=[e_1,e_2,\ldots,e_n]$ are the eigenvectors of S corresponding to the eigenvalues in $D=diag(\lambda_1, \lambda_2,\ldots, \lambda_n)$, respectively. To reduce the dimension of feature space, we adopted a significance-based PC selection method to choose a subset instead of all principle components for modeling Bayesian classifiers. Instead of comparing eigenvalues as ordering index (variance-based PC selection), the selection criterion in this work was based on the two-sample *t*-test result in the projective space spanned with each eigenvector. The first k eigenvectors with highest t values were survived and used to be the basis of the projective space for model learning. The ratio of the first k eigenvalues associated with the selected k principle components means preservation of discriminating information in the original data. Here, we used the receiver operating characteristic (ROC) curve to compare the performance between the proposed significance-based method and the conventional variance-based method.

2.6 Model learning

The classification model in this work to be constructed was based on Bayes' rule:

$$P(C_i|x) = \frac{P(x|C_i)P(C_i)}{P(x)} \tag{4}$$

where x is the data to be evaluated and C_i is the category (BD or normal) with corresponding priors $P(C_i)$. The terms $P(C_i)$ and $P(x)$ could be directly estimated from training data. In this study, the prior $P(C_i)$ for BD group/normal groups were set as 0.165 and 0.835, respectively, because the amounts of BD patients/normal controls were 15 and 76. Instead of assuming the probability density/likelihood function $P(x|C_i)$ as a Gaussian distribution, we estimated the likelihood function by Parzen-window method as follows:

$$P(x) = \frac{1}{n}\sum_{i=1}^{n} \frac{1}{h}\phi\left(\frac{x - x_i}{h}\right) \tag{5}$$

where $\phi\left(\frac{x - x_i}{h}\right)$ is the window function with window size h:

$$\phi\left(\frac{x - x_i}{h}\right) = \begin{cases} 1, & |x - x_i| \le \frac{h}{2} \\ 0, & otherwise \end{cases} \tag{6}$$

Once the likelihood function had been estimated from training data, the posterior probability $P(C_i|x')$ for some test data x' would be calculated based on the Bayesian rule to provide the probability of subject x' belonging to a specific group C_i. Furthermore, we could make a decision that the test subject would belong to the group with maximal a posteriori value.

Note that all procedures after VBM analysis were done for each tissue, GM, WM, and CSF, respectively. Therefore we got three probabilities for each subject. To make a final prediction for performance evaluation, we combined the three results by choosing the maximum probability of being abnormal rather than emphasizing the result of a specific tissue.

3. Results

Figure 2 shows the *t*-map of GM volume loss of BD patients compared with normal subjects by VBM analysis. Significant GM volume loss was located at the frontal lobe (including precentral, inferior and middle frontal gyrus),

parietal lobe (including postcentral and inferior parietal gyrus), and insula. On the other hand, significant WM volume increase was detected in the temporal lobe (including inferior, superior and middle temporal gyrus), frontal lobe (including inferior and middle frontal gyrus), thalamus, basal ganglia (including lentiform nucleus and putamen), and left cerebellum anterior lobe.

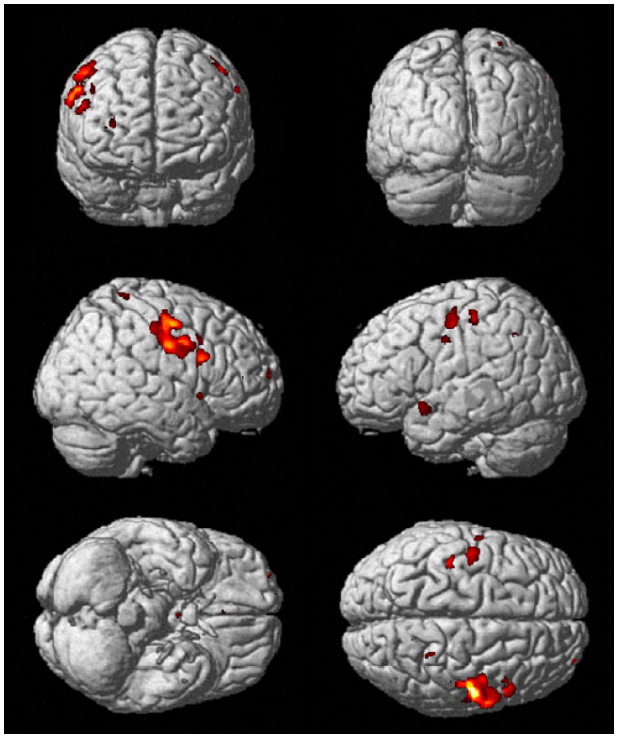

Figure 2. Volumetric atrophy of BD patients in gray matter analyzed by VBM analysis.

In this study, the clinical diagnosis from professional physicians was considered as the ground truth. The classification accuracy was then evaluated by comparing predictions with the ground truth. We adopted leave-one-out cross-validation method to report our accuracy. Figure 3 illustrates the prediction results of all subjects. It shows that most of the healthy controls had low probabilities of belonging to bipolar disorder. On the other hand, most of BD patients had relatively high predicted probabilities. This result demonstrated the reliability of the proposed method for the diseased group. Figure 4 displays the predicted probabilities of all 15 BD patients from VBM results based on three different tissues, gray matter (GM), white matter (WM), and cerebrospinal fluid (CSF), respectively. The BD patients with indices from 1 to 5 are males, and the others are females. The maximum of three probabilities is chosen as the final prediction outcome. Overall, WM had the most distinguishing characteristic among the three tissues.

In addition to classification accuracy, we also used false-positive (FP) and false-negative (FN) rates to evaluate system performance in terms of total minimal risk. FP, also called false alarm, means that the result predicted that a subject belonged to BD, but actually the subject did not. FN, also called misdetection, means that the result predicts that a subject did not belong to some disorder, but actually the subject did. Although both FP and FN represent incorrect classification result, the costs of these two errors are quite different. Thus, in this work, we defined the risk of a false alarm as 1 and the risk of a misdetection as 1.5. The variance ratios used in GM, WM, and CSF classifiers were 10%, 80%, and 60%, respectively. The results showed that the FN and FP rates were 0% and 15.8%, respectively, and the classification accuracy based on minimal risk criterion was 86.8%.

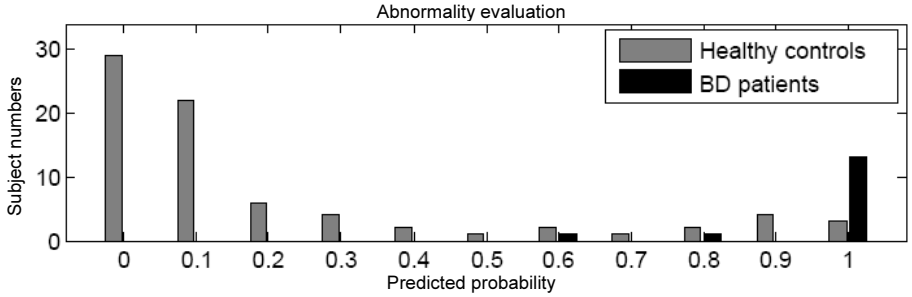

Figure 3. Histogram of predicted probability for all subjects.

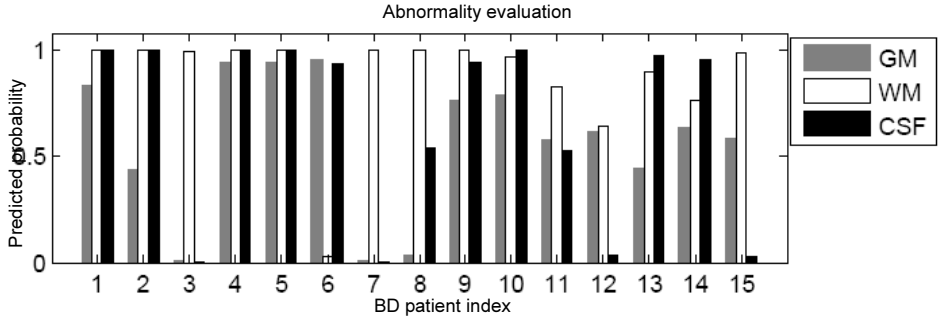

Figure 4. The predicted probabilities of all 15 BD patients from VBM results based on three different tissues, gray matter (GM), white matter (WM), and cerebrospinal fluid (CSF), respectively. The BD patients with indices from 1 to 5 are males, and the others are females.

4. Discussion

4.1 Structural discrepancy between BD patients and normal subjects

Comparing brain structural differences between BD patients and normal subjects, significant volume loss was located at the frontal lobe (including precentral, inferior and middle frontal gyrus), parietal lobe (including postcentral and inferior parietal gyrus), insula, lateral ventricle, and third ventricle. Several studies showed that phenomena of concentration or volume loss in the frontal lobe appeared in brain structures of BD patients. However, two unreasonable results, the lateral ventricle and third ventricle, were found and inconsistent with the literature. The results may be due to small sample population, so that each subject had large contribution to the statistical analysis.

On the other hand, significant volume increase was detected in the temporal lobe (including inferior, superior and middle temporal gyrus), frontal lobe (including inferior and middle frontal gyrus), thalamus, basal ganglia (including lentiform nucleus and putamen) and left cerebellum anterior lobe in this work. Some published studies revealed the volume increase of the temporal lobe, thalamus, and basal ganglia, though some had opposite results. Nevertheless, there was no clear pathological discovery in brain structures of BD patients. Therefore, these detected significant regions were entirely used for ROI selection followed by feature extraction for classification in this study.

4.2 Dimension reduction of feature space

A well-known phenomenon, termed the curse of dimensionality (small sample size problem), describes relations between the finite training data and the number of features. It refers to the problem that adding extra dimensions to a space would cause the exponential growth of hypervolume. In a classifier design, this problem may lead to the peaking phenomenon and affect the performance of the classifier. In practice, it is often observed that adding features may result in a poor outcome of a classifier if the number of features is large relative to that of training samples used for classification. Therefore, it is essential to have the training data with a reasonable sample size for selecting reliable features.

In this study, we encountered the small sample size problem. The number of features was much larger than the number of training samples (participants), even if ROIs were selected. It not only caused the result to lack stability but also cost high computation time. In order to deal with this problem, features extracted from ROIs were applied in the significance-based PC selection method to search for the most similar data representation in a lower-dimension space.

4.3 Comparison between significance-based PC selection method and variance-based PC selection method

PCA is a linear transformation technique that simplifies a data set. It preserves the characteristics of a data set in a high-dimensional space and projects it into an condensed and lower-dimensional representation for analysis. We repeated the whole procedure to check the performance of variance-based PC selection method. In other words, we ordered eigenvectors by their corresponding eigenvalues decreasingly as usual. We then got a lower classification accuracy of 76.9% in BD analyses. That is because PCA finds the projection which was well suited to only the whole data set but not suited to characteristics of several clusters. Thus, the significance-based PC selection method is more suitable to data composed of several clusters. That is to say, such a criterion is more suitable to classification purpose.

In this study, we used ROC curve to evaluate the performance of these two PC selection methods, significance-based and variance-based approaches. We varied the variance ratio from 10% to 100% for all tissues: GM, WM, and CSF, and then there were 1000 combinations to determine characteristics of the final classifiers. Figure 5 illustrates ROC curves of the BD classifier with these two PC selection methods. A curve fitting method was applied to fit the rough results result from small sample size. It shows that the ROC curve of the significance-based PC selection method was closer to the top left corner than the traditional variance-based PC selection method. The corresponding PAUC index of significance-based PC selection method was 83.6%, which was larger than that of variance-based PC selection method, 78.4%. It demonstrated that the significance-based PC selection criterion would achieve a better classification performance.

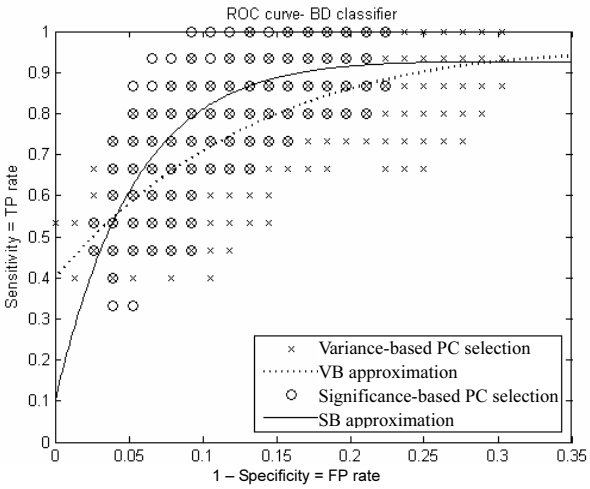

Figure 5. ROC curves of two PC selection methods. The crosses are the classification results of variance-based (VB) PC selection method, and the dotted line is the fitting curve. The circles are the classification results of significance-based (SB) PC selection method, and the solid line is the fitting result.

4.4 Size of Parzen window

In the Parzen-window density estimation approach, the parameter, window size, plays an important role in the classification model. The estimated density function will be smoothed over if the window size is too large, and noisy if it is

too small. It means we will have inaccurate density estimation if an improper window size is used. Furthermore, an inaccurate estimated density function will lead to a poor outcome of the posteriori probability and make an incorrect prediction of a classification system. Thus, it is critical to choose the proper window size. In this study, we decided the window size by visual inspection of estimated density function distributions instead of trying lots of values to find a better classification results.

To find a proper size of Parzen window, we chose the first two principle components as axes to form a coordinate system and projected the data into this new space. Then, we sketched the projected distribution and the density function of two groups in different window sizes varying from 1 to 8. According to the variations of density function in each kind of window size, we could easily estimate the suitable window size by visualization. Figure 6 shows the results of different window size. We can see that both distributions of normal and BD subjects are smooth enough when the window size equals 5. Therefore, window size was set as 5 to estimate the density function for all GM, WM, and CSF classifiers in this study.

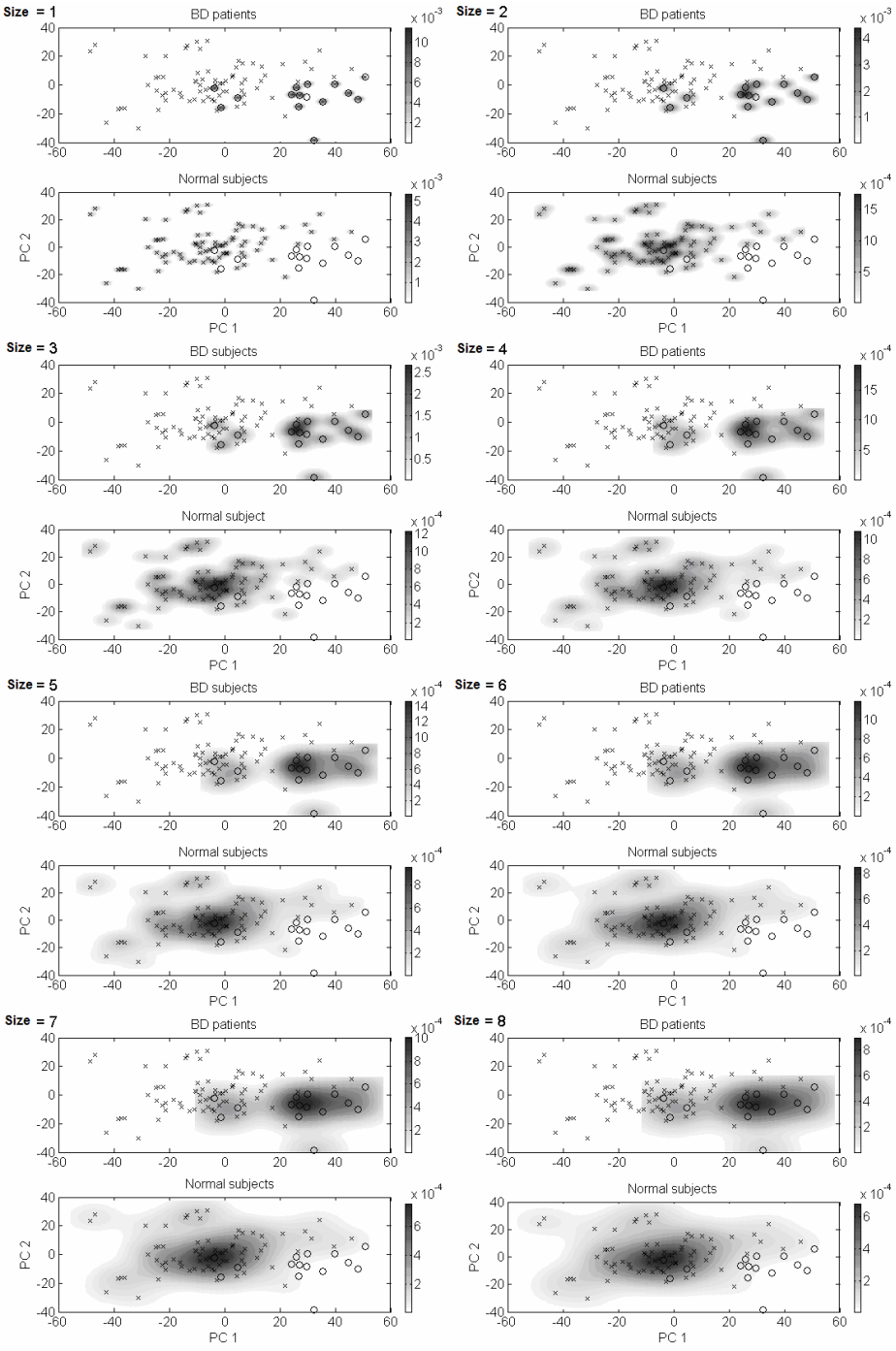

Figure 6. Visualization of density functions in varying the window size. The crosses are the distribution of the normal group, and the circles are that of the BD group. For each window size, the above graph is the density function of the BD group and the below one is that of normal group.

5. Conclusions

This work has proposed a novel computer-aided evaluation system for bipolar disorder using anatomic MRI to provide a second opinion for clinical diagnosis. We adopted the VBM method to identify brain regions with significant difference between BD patient and normal control groups as ROIs followed by feature extraction with significance-based PCA approach. The classification model based on Bayesian theorem together with Parzen-window density estimation in PCA space was constructed to provide the probability of an individual belonging to the BD patient group. In our experiment, the proposed system reached 86.8% accuracy in classification. The misdetection rate was zero and the false alarm rate was 15.8%. It demonstrated that the proposed computer-aided system could detect the disease of bipolar disorder and obtain high classification accuracy.

Acknowledgements

This work was partially supported by National Science Council, Taiwan, under Grant NSC 96-2752-B-075-001-PAE and Taipei Veterans General Hospital under Grant VGH V96ER1-003.

References

[1] M. L. Phillips and E. Frank, "Redefining bipolar disorder: toward DSM-V," *Am. J. Psychiat.*, 163: 1135-1136, 2006.

[2] P. J. Pardo, A. P. Georgopoulos, J. T. Kenny, T. A. Stuve, R. L. Findling and S. C. Schulz, "Classification of adolescent psychotic disorders using linear discriminant analysis," *Schizophr. Res.*, 87: 297-306, 2006.

[3] Z. Lao, D. Shen, Z. Xue, B. Karacali, S. M. Resnick and C. Davatzikos, "Morphological classification of brains via high-dimensional shape transformations and machine learning methods," *Neuroimage*, 21: 46-57, 2004.

[4] Y. Fan, H. Rao, J. Giannetta, H. Hurt, J. Wang, C. Davatzikos and D. Shen, "Diagnosis of brain abnormality using both structural and functional MR images," *Conf. Proc. IEEE Eng. Med. Biol. Soc.*, Suppl.: 6585-6588, 2006.

[5] Y. Kawasaki, M. Suzuki, F. Kherif, T. Takahashi, S. Y. Zhou, K. Nakamura, M. Matsui, T. Sumiyoshi, H. Seto and M. Kurachi, "Multivariate voxel-based morphometry successfully differentiates schizophrenia patients from healthy controls," *Neuroimage*, 34: 235-242, 2007.

[6] U. Yoon, J. M. Lee, K. Im, Y. W. Shin, B. H. Cho, I. Y. Kim, J. S. Kwon and S. I. Kim, "Pattern classification using principal components of cortical thickness and its discriminative pattern in schizophrenia," *Neuroimage*, 34: 1405-1415, 2007.

[7] J. Ashburner and K. J. Friston, "Voxel-based morphometry-the methods," *Neuroimage*, 11: 805-821, 2000.

[8] C. D. Good, I. S. Johnsrude, J. Ashburner, R. N. Henson, K. J. Friston and R. S. Frackowiak, "A voxel-based morphometric study of ageing in 465 normal adult human brains," *Neuroimage*, 14: 21-36, 2001.

[9] E. R. Sowell, P. M. Thompson, S. E. Welcome, A. L. Henkenius, A. W. Toga and B. S. Peterson, "Cortical abnormalities in children and adolescents with attention-deficit hyperactivity disorder," *Lancet*, 362: 1699-1707, 2003.

[10] J. Pujol, C. Soriano-Mas, P. Alonso, N. Cardoner, J. M. Menchon, J. Deus and J. Vallejo, "Mapping structural brain alterations in obsessive-compulsive disorder," *Arch. Gen. Psychiatry*, 61: 720-730, 2004.

[11] S. Y. Yoo, M. S. Roh, J. S. Choi, D. H. Kang, T. H. Ha, J. M. Lee, I. Y. Kim, S. I. Kim and J. S. Kwon, "Voxel-based morphometry study of gray matter abnormalities in obsessive-compulsive disorder," *J. Korean Med. Sci.*, 23: 24-30, 2008.

[12] A. A. Valente, Jr., E. C. Miguel, C. C. Castro, E. Amaro, Jr., F. L. Duran, C. A. Buchpiguel, X. Chitnis, P. K. McGuire and G. F. Busatto, "Regional gray matter abnormalities in obsessive-compulsive disorder: a voxel-based morphometry study," *Biol. Psychiatry*, 58: 479-487, 2005.

[13] I. J. Osuji and C. M. Cullum, "Cognition in bipolar disorder," *Psychiatr. Clin. North Am.*, 28: 427-441, 2005.

[14] Y. I. Sheline, "Neuroimaging studies of mood disorder effects on the brain," *Biol. Psychiatry*, 54: 338-352, 2003.

[15] S. M. Strakowski, M. P. DelBello, C. Adler, D. M. Cecil and K. W. Sax, "Neuroimaging in bipolar disorder," *Bipolar Disord.*, 2: 148-164, 2000.

[16] S. D. Bruno, G. J. Barker, M. Cercignani, M. Symms and M. A. Ron, "A study of bipolar disorder using magnetization transfer imaging and voxel-based morphometry," *Brain*, 127: 2433-2440, 2004.

[17] X. Chen, W. Wen, G. S. Malhi, B. Ivanovski and P. S. Sachdev, "Regional gray matter changes in bipolar disorder: a voxel-based morphometric study," *Aust. N. Z. J. Psych.*, 41: 327-336, 2007.

[18] A. C. Nugent, M. P. Milham, E. E. Bain, L. Mah, D. M. Cannon, S. Marrett, C. A. Zarate, D. S. Pine, J. L. Price and W. C. Drevets, "Cortical abnormalities in bipolar disorder investigated with MRI and voxel-based morphometry," *Neuroimage*, 30: 485-497, 2006.

[19] H. Scherk, C. Kemmer, J. Usher, W. Reith, P. Falkai and O. Gruber, "No change to grey and white matter volumes in bipolar I disorder patients," *Eur. Arch. Psych. Clin. Neurosci.*, 258: 345-349, 2008.

[20] J. Z. Konarski, R. S. McIntyre, S. H. Kennedy, S. Rafi-Tari, J. K. Soczynska and T. A. Ketter, "Volumetric neuroimaging investigations in mood disorders: bipolar disorder versus major depressive disorder," *Bipolar Disord.*, 10: 1-37, 2008.

[21] A. Fornito, G. S. Malhi, J. Lagopoulos, B. Ivanovski, S. J. Wood, M. M. Saling, C. Pantelis and M. Yucel, "Anatomical abnormalities of the anterior cingulate and paracingulate cortex in patients with bipolar I disorder," *Psychiatry Res.*, 162: 123-132, 2008.

[22] R. A. Lochhead, R. V. Parsey, M. A. Oquendo and J. J. Mann, "Regional brain gray matter volume differences in patients with bipolar disorder as assessed by optimized voxel-based morphometry," *Biol. Psychiatry*, 55: 1154-1162, 2004.

[23] S. M. Smith, M. Jenkinson, M. W. Woolrich, C. F. Beckmann, T. E. Behrens, H. Johansen-Berg, P. R. Bannister, M. De Luca, I. Drobnjak, D. E. Flitney, R. K. Niazy, J. Saunders, J. Vickers, Y. Zhang, N. De Stefano, J. M. Brady and P. M. Matthews, "Advances in functional and structural MR image analysis and implementation as FSL," *Neuroimage*, 23 Suppl. 1: S208-219, 2004.